CORPUS PUBLISHERS

Journal of Mineral and Material Science (JMMS)

Volume 3 Issue 3, 2022

Article Information

Received date :August 05, 2022

Published date: August 15, 2022

*Corresponding author

Camila Pacelly Brandão de Araújo, Sciences and Technology School, Universidade Federal do Rio Grande do Norte UFRN, 59.078-970, Rio Grande do Norte, Brazil

Keywords

Kinetic Data; Tungsten Carbide; Gas-Solid Reaction

Research Article

Evaluation of Kinetic Data of the WC's Synthesis Via Gas-Solid Reaction

Camila Pacelly Brandão de Araújo[1], Amanda Araújo Gomes da Silva[1], Laércio Martins de Mendonça Filho[1] and Carlson Pereira de Souza[2]

[1]Sciences and Technology School, Universidade Federal do Rio Grande do Norte UFRN, 59.078-970, Rio Grande do Norte, Brazil

[2]Chemical Engineering Department, Laboratório de Materiais Nanoestruturados e Reatores Catalíticos, Universidade Federal do Rio Grande do Norte /UFRN, 59.0 78-970, Rio Grande do Norte, Brazil

Abstract

Tungsten carbide (WC) stands out in the mechanical industry, chemical and aerospace by presenting a unique combination of properties, such as high hardness, high melting point, high wear resistance, great chemical, and thermal stability. Refractory carbides' synthesis via gas-solid reaction is an interesting processing route as it can produce those materials in nanoscale and thus, enhance several of its properties. In this paper, the WC production process was studied upon the evaluation of kinetic data available in the literature. The synthesis data were obtained through the "Digitize" tool of the Origin® software and two kinetic models were evaluated regarding its agreement with those data: 1st order powerlaw and Avrami model. Kinetic constants using a 1st order reaction were estimated and a $k=0.00181 min^{-1}$ with $R^2=0.9646$ for the reaction at 850 °C and 120min of soaking time.

Introduction

The development of new materials or the improvement of the set of properties of well-known materials using different synthesis' routes is one of the main driving forces of materials engineering. If, in addition, said materials have versatile applications, then materials engineers are in their most important working field. Refractory carbides are compounds in which carbon atoms combine with refractory metals forming a structure that presents properties of both metals and ceramics, which is a unique characteristic of this type of material [1]. The use of refractory carbides is wide and are versatile, as they present applications in many different fields, such as hard and powder metallurgy, automotive, oil extraction and refining, manufacturing, and others [2-4]. One of the most important features playing a role in carbide's properties is the applied processing [1,5]. Various methodologies can be used for this purpose: high-energy milling [6] plasma, chemical vapour deposition, among others. By changing this it is possible to obtain materials with different characteristics, including particle size, phase distribution, and surface area [7]. The route traditionally employed for the synthesis of tungsten carbide derives from the metallurgy where carbon black a source of metallic W, mainly tungstic acid, Blue Tungsten Oxide (TBO), or ammonium tungstate [7] are led to react in a reductive hydrogen atmosphere inside a graphite oven, between 1400–1800 °C, with long reaction times. In this process, three main reaction stages can be identified: carbon adsorption onto metallic tungsten, carbon diffusion into the tungsten matrix, followed by nucleation and growth of the carbide phase [8,9]

The carbide synthesis via gas-solid reaction can overcome several constraints present in other processes, namely obtaining the materials using lower temperatures and reaction times, with high control over their size, shape, and structure [4,7].

Despite the vast research dedicated to obtaining these materials using various carbon sources [10-12], each with its own set of reaction parameters (time and temperature), there have been few studies dedicated to the evaluation of kinetic parameters of this process. This type of study is of fundamental importance to the scale-up of any bench process to a pilot plant, as well as the economic viability of the process on an industrial scale. A kinetic study aims to analyze and characterize the various factors that influence the reaction rate and propose a mechanism that can explain the process. Several variables may affect the reaction rate, thus it is necessary to consider the nature of the reaction, the number of phases involved, as well as the presence of catalysts. Kinetic studies for carbide synthesis investigate, for instance, the production of TiC via calciothermic reduction in an argon atmosphere [13] NbC from Nb_{2O5} from two methodologies, namely rotary cylinder, and a fixed bed reactor [14,15], and the non-isothermal synthesis of WC from metallic W and methane using the Joule effect [16]. Concerning the WC synthesis, [17] attained pure WC after 60min of reaction at 850 °C using a heterogeneous gas-solid reaction, with CH4 and H_2 gas mixture in a fixed bed reactor. Further investigation revealed that the reaction rate was dependent on the initial load of W precursor (TBO or APT), the composition, and the flow rate of the gas phase. These observations agree with the previous reports by [18]. In their work, [9] used different processing conditions for this gas-solid reaction, showing the rate of consumption of the gas phase (methane consumption) for each of them, however, no kinetic data was effectively obtained from this. Therefore, the presented work proposes the evaluation of those data, so that kinetic parameters may be estimated for this process and a scale-up of it can be done. Kinetic data were evaluated using both the first-order power model and Avrami's models.

Power-Law Model

The simplest kinetic model assumes that the reaction rate is directly proportional to the product of the concentration of the reagents. Considering the general reaction (Equation 1) A and B molecules must collide to react, and the probability of thus collisions producing products is proportional to the product of its concentrations [19].

$$aA + bB \rightarrow cC + dD$$

Equation 1

The rate equation can be written according to the Power-Law Model (Equation 2)

$$r_A = k(T)[A]^n[B]^m \quad \text{Equation 2}$$

Where k(T) is the proportionality constant called the speed constant, [A] and [B] are the concentrations of the reagents. The magnitude of k varies with temperature, so it determines how the temperature influences speed of the reaction. Exponents n and m are known as reaction orders and indicate how the speed is affected by the concentration of each reagent. The total order of the reaction is the sum of the orders of each reagent in the rate law.

Nucleation and growth model

Nucleation and growth models e widely used in Materials Engineering and Crystallization processes for producing crystalline salts from a concentrated solution. The nucleation and growth model proposed by [20] is based on the activation of reaction sites followed by the growth of product cores after an induction period. It proposes that a system is capable of phase transformation once it is composed of embryos of the new phase. Such embryos or nucleotides consist of random and transient arrangements of molecules, inherent in the preparation process or formed due to specific heat treatments, with compositions close to those of the molecules of the new phase. When the phase change begins, some of these embryos begin to grow, acquiring thermodynamic stability and not dissolving, and reach a critical size and become nuclei. In this process, the number of embryos goes down over time as they become nuclei or are absorbed by growing nuclei. In this way, the formation of the new phase occurs due to the agglomerations of growing nuclei [13,15,16]. Figure 1 presents the steps related to the Nucleation and Growth model in an illustrative way.

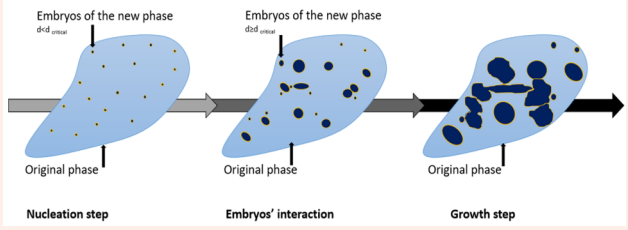

Figure 1: Nucleation and growth model illustrative description.

This model, although elaborated for crystallization kinetics of solids in a liquid (melt) phase, can be applied, in general, to any phase transformation. Therefore, it applies to chemical reactions involving fluid-particle interaction. Equation 3 shows the time-conversion relation to this case. When a given process fits this model a linear adjustment to Equation 4 is obtained. Equation 4 shows the double application of the logarithm function to Equation 3 producing a straight-line equation.

$$x = 1 - e^{-Mt^N} \quad \text{Equation 3}$$

$$\ln\left[\ln\left(\frac{1}{1-x}\right)\right] = \ln(M) + N\ln(t) \quad \text{Equation 4}$$

Where x is the mass fraction of the new phase after a time t, N is the Avrami exponent, which depends on the growth mechanism and dimensionality of the crystal, and M is the kinetic constant defined as the effective reaction rate.

Materials and Methods

A- Data acquisition

The digitizer tool of the Origin® Software was used to acquire methane consumption data over time on several reaction conditions (presented in Table 1) for the synthesis of WC. Those data, presented in the work of [17] were acquired by using an FID detector on chromatography equipment on the exit gas stream of a fixed bed reactor, according to the apparatus presented in Figure 2. Samples were analyzed every three minutes and it was possible to evaluate methane consumption throughout reactions.

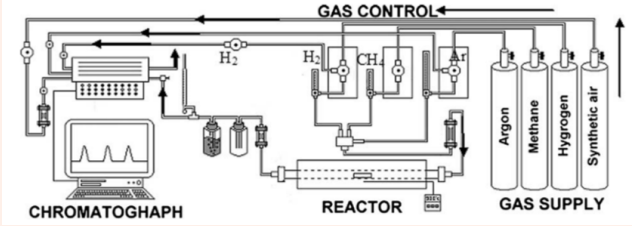

Figure 2: Apparatus used by [17] for the evaluation of WC's synthesis via gas-solid reactions.

Table 1: Reaction conditions examined. B- Data treatment.

Name	T (°C)	Q (L/min)	%CH_4	m (g)	Particle size
R1	850	17	5	2	As received
R2	800	17	5	2	As received
R3	850	17	5	2	As received
R4	850	17	5	3	As received
R5	850	30	5	4	Sieved (#400)

Plotted graphics of such consumption were published on the referred paper and, were later acquired by these authors by manually choosing point-by-point gas consumption percentage versus reaction time. Though methane consumption data were presented in arbitrary units by those authors, these authors chose to evaluate it on a percentage basis. Therefore, a baseline was established (initial methane consumption). This point was chosen to be the average of the five first points of the chromatographic exit evaluation. It was considered that at that condition no reaction had yet taken part and a mass balance would show, according to Equation 5, that that measurement equaled that of the initially fed methane, as a steady-state condition would.

$$F_{CH4\,in} - F_{CH4\,out} = \frac{d\%CH_4C}{dt} \quad \text{Equation 5}$$

Therefore: $$F_{CH4\,in} - F_{CH4,0} = \frac{\%CH_{4,0}.Q_{CH4}.P}{RT} \quad \text{Equation 6}$$

Where FCH_4 is the methane molar flow rate (mol/s), P is the reactor pressure (atmospheric pressure), QCH_4 is methane volume flow rate (L/min), T is the reaction temperature (K) and R is the ideal gas constant (8.314 J/mol.K). % CH_4,0 was considered 100%. During the reaction, the methane output could differ from its initial input due to the main reaction occurring, Equation 7 was used to calculate its molar flow rate.

$$F_{CH4,t} = \frac{(\%CH_{4,t} - \%CH_{4,0})Q_{CH4}.P}{RT} \quad \text{Equation 7}$$

1st Order Power Law Model

Those data were used in the integrated rate law, Equation (8) to evaluate the agreement of the first-order kinetic model for this process.

$$\ln C_{CH4,t} = -kt - \ln C_{CH4,0} \quad \text{Equation 8}$$

Where $C_{CH4,0}$ and $C_{CH4,t}$ are the initial and instantaneous methane concentrations, respectively given by Eqs. 9 and 10, respectively.

$$C_{CH4,0} = (\%CH_{4,0})Q_{CH4} \quad \text{Equation 9}$$

$$C_{CH4,t} = \left(\%CH_{4,t}\right) Q_{CH4}$$ Equation 10

The kinetic rate constant was determined using Equation (8), by plotting the methane concentration with time for all conditions established in Table 1.

Avrami's Model

Equations 3 and 4 show the time-conversion relation when Avrami's Model is applied. Those equations were used considering that X, which is the mass fraction of the new solid phase after a time t, could be estimated by the reaction stoichiometric coefficients. The reaction between APT and the gaseous mixture of methane - hydrogen can be described by the stoichiometric equations of APT decomposition (Equation 11), reduction of tungsten trioxide (Equation 12), and tungsten carburization (Equations 13 and 14) according to several authors [17,18,21].

$$(NH_4)_{10}(H_2W_{12}O_{42}) \cdot 4H_2O \;\bar{\Delta}\; 12WO_3 + 10H_2O + 10NH_3$$ Equation 11

$$WO_3 + 3H_2 \rightarrow W + 3H_2O$$ Equation 12

$$2W + CH_4 \rightarrow W_2C + 2H_2$$ Equation 13

$$W_2C + CH_4 \rightarrow 2WC + 2H_2$$ Equation 14

When chemical reactions occur in multiple steps, the slowest step controls the overall rate of the reaction. This step, called the rate-determining step, governs the reaction rate. According to [17], for this process, the rate-determining step is the second step of tungsten carburization. The results of the studies by other authors [11,18,22] agree with De Medeiros' conclusion and, therefore, the focus of the kinetic analysis was the conversion of the solid phase from W_2C to WC.

By reaction stoichiometry (Equation 14), one can observe a direct proportion between the methane consumption and the formation of W_2C. That is, when 1 mol of methane is consumed, 1 mol of W_2C is also consumed to produce 2 WC moles. Therefore, it was considered that all the methane consumed in the reactor during the time interval considered (2nd step of the carburization – Equation 14), was used in the formation of the WC phase.

Methane molar flow data were converted into a solid conversion fraction using Equation 19:

$$x = \frac{N_o - N_f}{N_0}$$

Where X is the converted fraction of solid, N_o is the initial molar flow, and N_f is the molar flow in the instant of time t. Thus, the conversion of the solid was calculated at each moment of the reaction. These conversion data were used in the Avrami model (Equations 2 and 3) to determine the effective reaction rate (M) and Avrami's exponent (N).

Results and Discussion

1st Order Power Law Model

Figures 3-7 show the use of the 1st order power-law model over the experimental data and its linear fit. In Table 2, the attained k values and corresponding correlation coefficients are presented. Throughout the reactions, an average correlation coefficient (R^2) of 0.904 was calculated, this demonstrates the good agreement between model and experimental data. All specific correlation coefficients were found to lie very close to the average, except for reaction 2, which presents the largest of the deviations (R^2=0.7665). However, reaction 2 was originally performed at 800 °C, and, in this condition, [17] found by X-Ray Diffraction that approximately 10% in weight of W_2C was still found in the powders synthesized, [22] also found the W_2C incomplete carburation at 900-1000 K temperature in the reaction between WO_3 and H_2-CH_4 with 60 and 120min soaking times and attributed this to the slow carbon supply given by the gas phase and its diffusion in the solid. This incomplete W_2C conversion could be the reason why the 1st order model could not fully and suitably explain the phenomena. Disregarding this reaction, the arithmetic average of the correlation coefficient rises to 0.937 and presents its highest value in reaction 4 (R^2>0.96). Upon comparing the kinetic parameters of reactions 1 and 4, an increase of 94% in the reaction rate constant can be observed. This could be attributed to the increased gas flow, which caused an increase in carbon availability, thus leading to higher reaction rates, as the basic requirement for the complete conversion of W_2C is the appropriate carbon availability.

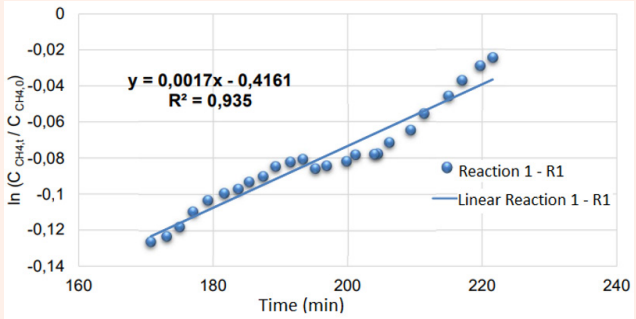

Figure 3: Linear fit of the 1st order power law model to experimental data from Reaction 1: Flow rate=17L/h, %CH4=5, Temperature=850 °C, APT weight=2g.

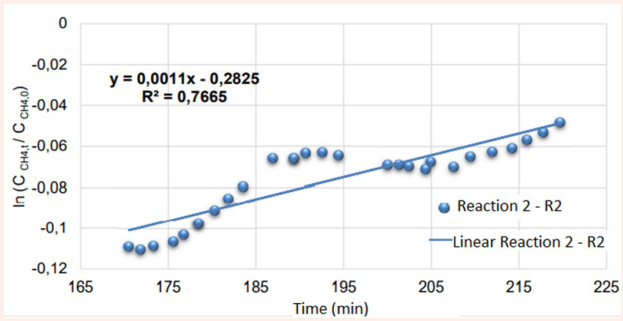

Figure 4: Linear fit of the 1st order power law model to experimental data from Reaction 2: Flow rate=17L/h, %CH4=5, Temperature=800 °C, APT weight=2g.

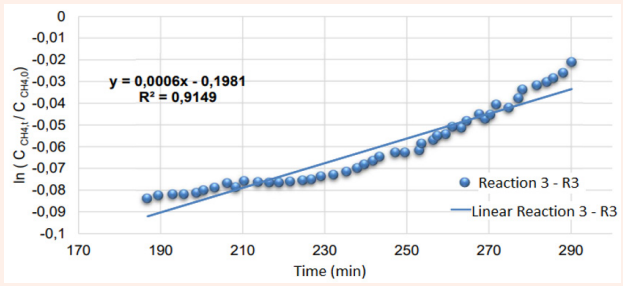

Figure 5: Linear fit of the 1st order power law model to experimental data from Reaction 3: Flow rate=17L/h, %CH4=5, Temperature=850 °C, APT weight=4g.

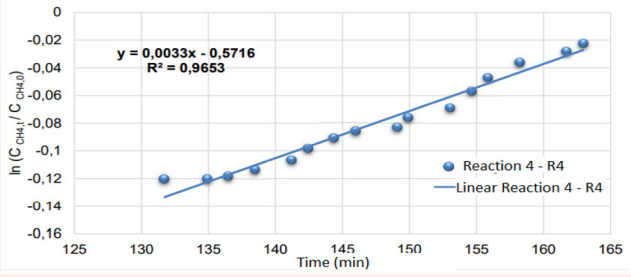

Figure 6: Linear fit of the 1st order power law model to experimental data from Reaction 4: Flow rate=30L/h, %CH4=5, Temperature=850 °C, APT weight=3g.

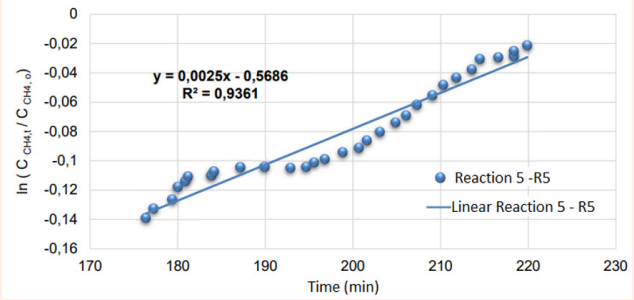

Figure 7: Linear fit of the 1st order power law model to experimental data from Reaction 5: Flow rate=17L/h, %CH4=5, Temperature=850 °C, APT weight=g, sieved (#400).

Table 2: Correlation coefficients obtained using 1st order power law-model.

Reaction	K (min^{-1})	R^2
R1	0,0047	0,935
R2	0,0011	0,767
R3	0,0006	0,915
R4	0,0033	0,965
R5	0,0025	0,936
Average	0,0018	0,904

On the other hand, upon increasing the APT load (Figures 3 & 5) a 35% reduction in the reaction rate constant can be observed. Duly so, observing Figures 3 & 5, there is a delay of approximately 30min for begin of the decrease and stabilization of methane conversion. This is evidence of greater difficulty in obtaining WC. The increase in the reactor load increases the path for carbon diffusion, which impairs reaction. The reduction in granulometry provided an increase of 47% in the kinetics when compared to the first reaction (R1). In terms of the phenomena, the reduction in the powder's granulometry provides shorter diffusion paths for C in the solid, as well as a larger surface area for better C absorption [22].

In summary, the values of the kinetic constant found by the adjustment of 1st order indicate that the reaction rate has been increased by increasing the flow of methane (k_{R4}=0.0033min^{-1}), refinement in precursor granulometry (k_{R5}=0.0025min^{-1}), the reduction of the precursor load (k_{R1}=0.0017min^{-1} and k_{R3}=0.0006min^{-1}) and temperature increase (k_{R1}=0.0017min^{-1} and k_{R2}=0.0011min^{-1}). This agrees with [17] analysis of the physical phenomena.

Avrami's Model

Figures 8-12 present the adjustment of the experimental data to the Avrami nucleation and growth model. Avrami's exponent (N) and the kinetic constant (M) were determined by the linearization of the conversion fraction versus time (Equation 4) and those values were determined from the angular and linear coefficient of the ln[-ln(1 – x)] versus ln(t). They are gathered in Table 3. Correlation coefficients (R^2) for Avrami's model presented an arithmetic mean of 0.878, demonstrating decreased adequacy to the data in comparison to the data adjustment provided by the 1st order Power Law Model (mean R^2>0.90). Effective reaction rate (M) values indicate the influence of each of the processing parameters analyzed. The gas flow was the parameter that seem to have the greater influence upon the reaction rate. This can be justified by the increased availability of carbon on the solid's surface. The order of influence over the reaction rate was then followed by the reduction in solid granulometry, reduction of APT load, and temperature increase.

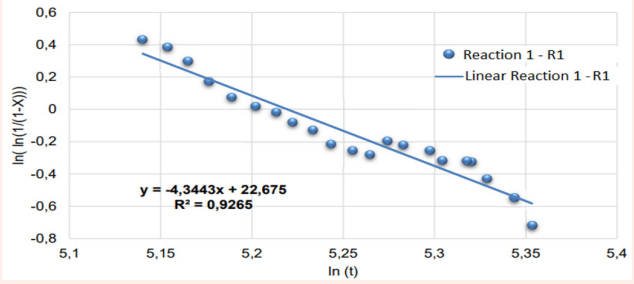

Figure 8: Avrami's model adjustment to experimental data for Reaction 1: : Flow rate = 17 L/h, %CH4 = 5, Temperature =850°C, APT weight = 2g.

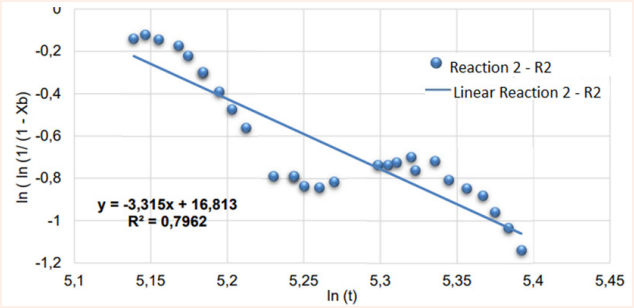

Figure 9: Avrami's model adjustment to experimental data for Reaction 2: Flow rate=17L/h, %CH4=5, Temperature=800 °C, APT weight=2g.

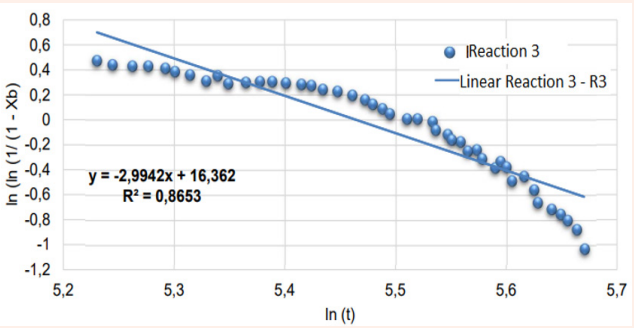

Figure 10: Avrami's model adjustment to experimental data for Reaction 3: Flow rate=17L/h, %CH4=5, Temperature=850 °C, APT weight=4g.

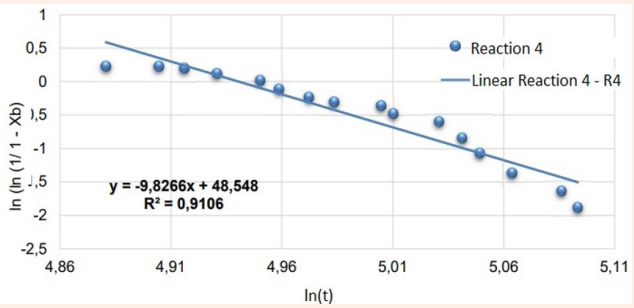

Figure 11: Avrami's model adjustment to experimental data for Reaction 4: Flow rate=30L/h, %CH4=5, Temperature=850 °C, APT weight=3g.

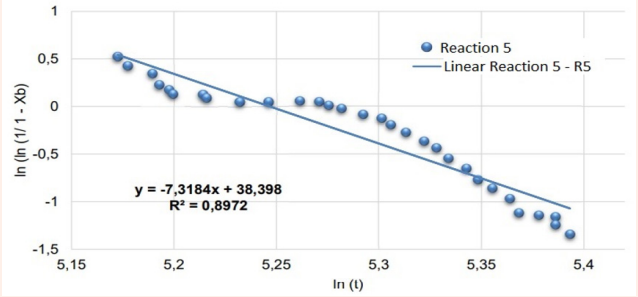

Figure 12: Avrami's model adjustment to experimental data for Reaction 5: Flow rate=17L/h, %CH4=5, Temperature=850 °C, APT weight=g, sieved (#400).

Table 3: Correlation coefficients obtained using Avrami's model.

Reaction	Ln (M)	N	R^2
R1	22.675	4.344	0.936
R2	16.183	3.315	0.796
R3	16.362	2.994	0.865
R4	48.548	9.827	0.911
R5	38.398	7.318	0.897
Average	28.559	5.56	0.878

According to [23], the critical steps for the formation of the WC are the formation of active carbon C* on the W surface and its diffusion in the metallic W. The parameters analyzed directly influence these steps: the reduction of granulometry provides an increase in the surface area available for carbon interact with w; the increase in temperature causes an increase in the diffusion rate, and the reduction in mass decreases the path to be traveled to the complete conversion of the solid.

Conclusion

The first order power law model was of greater suitability in explaining the experimental data (R^2>0.90) than the Avrami Model for the synthesis of tungsten carbide via gas-solid reaction in methane and hydrogen atmosphere. According to the calculations, the extent of the influence of each of the following parameters increase in the order: methane flow (k_{R4} = 0.0033min^{-1}), precursor granulometry (k_{R5}=0.0025min^{-1}), reduction of precursor load (k_{R1}=0.0017min^{-1} and k_{R3}=0.0006min^{-1}) and temperature (k_{R1}=0.0017min^{-1} and k_{R2}=0.0011min^{-1}). Correlation coefficients (R^2) for Avrami's model presented an arithmetic mean of 0.878, demonstrating lower adequacy to the data in comparison to the 1st order adjustment of the power law. The Avrami exponent (N) values found ranged from 2.99 to 9.83, with an arithmetic mean of 5.56. This indicates that the nucleation and growth process can occur by more than one mechanism. Reactions 1, 4, and 5 showed N greater than 4, indicating that growth is controlled by the transformation of polymorphic ($W_2C \rightarrow WC$), while the phase growth of reactions 2 and 3 is controlled by diffusion (N >2.5). The temperature increase (800 °C to 850 °C), the use of precursors with finer granulometry (Refined APT with sieve #400), and reduction of the precursor mass (4g to 2g) are sufficient to facilitate the diffusion process to a point that the $W_2C \rightarrow WC$ to be the controlling step of the reaction.

Acknowledgment

These authors acknowledge all the support given by the National Council for Scientific and Technological Development (CNPq).

Bibliographic References

1. Pierson H (1996) Handbook of refradory carbides and nitrides: properties, characteristics, processing and applications, Noyes Publications, Westwood, New Jersey, US.
2. Ettmayer P (1989) Hardmetals and cermets. Annual Review of Materials Science 19: 145-164.
3. de Araújo CPB (2018) Mo oxides and carbides with addition of Co: study of the effect of the dopant addition methodology and the kinetics of obtaining by gas-solid reaction.
4. Fang ZZ, Wang X, Ryu T, Hwang KS, Sohn HY (2009) Synthesis, sintering, and mechanical properties of nanocrystalline cemented tungsten carbide - A review. International Journal of Refractory Metals and Hard Materials 27(2): 288-299.
5. Buchel KH, Moretto HH, Woditsch P (2000) Industrial Inorganic Chemistry. (2nd edn), Wiley-VCH, Germany.
6. Torres CDS, Schaeffer L (2010) Effect of high energy milling on the microstruture and properties of wc-ni composite. Materials Research 13(3): 293-298.
7. Liu K (2012) Tungsten carbide - processing and applications. (1st edn), Intechopen com.
8. Medeiros FFP, de Oliveira SA, de Souza CP, da Silva AGP, Gomes UU, et al. (2001) Synthesis of tungsten carbide through gas-solid reaction at low temperatures. Materials Science and Engineering A 315(1-2): 58-62.
9. de Medeiros FFP, da Silva AGP, de Souza CP, Gomes UU (2009) Carburization of ammonium paratungstate by methane: The influence of reaction parameters. International Journal of Refractory Metals and Hard Materials 27(1): 43-47.
10. Li S, Kim WB, Lee JS (1998) Effect of the reactive gas on the solid-state transformation of molybdenum trioxide to carbides and nitrides. Chemistry of Materials 10(7): 1853-1862.
11. Lofberg A, Frennet A, Leclercq G, Leclercq L, Giraudon JM (2000) Mechanism of WO_3 reduction and carburization in CH_4/H_2 mixtures leading to bulk tungsten carbide powder catalysts. Journal of Catalysis 189(1): 170-183.
12. Mo T, Xu J, Yang Y, Li Y (2016) Effect of carburization protocols on molybdenum carbide synthesis and study on its performance in CO hydrogenation. Catalysis Today 261: 101-115.
13. Bavbande DV, Mishra R, Juneja JM (2004) Studies on the kinetics of synthesis of TiC by calciothermic reduction of TiO_2 in presence of carbon. Journal of Thermal Analysis and Calorimetry 78: 775-780.
14. Fontes FAO, Sousa JF, Souza CP, Bezerra MBD, Benachour M (2011) Production Of Nbc from Nb_2O_5 in a rotating cylinder reactor: Kinetic study of reduction/carburization reactions. Chemical Engineering Journal 175: 534-538.
15. Teixeira Da Silva VLS, Schmal M, Oyama ST(1996) Niobium carbide synthesis from niobium oxide: Study of the synthesis conditions, kinetics, and solid-state transformation mechanism. Journal of Solid State Chemistry 123(1): 168-182.
16. Kharatyan SL, Chatylyan HA, Arakelyan LH (2008) Kinetics of tungsten carbidization under non-isothermal conditions. Materials Research Bulletin 43(4): 897-906.
17. de Medeiros FFP, da Silva AGP, de Souza CP, Gomes UU (2009) Carburization of ammonium paratungstate by methane: The influence of reaction parameters. International Journal of Refractory Metals and Hard Materials 27(1): 43-47.
18. Leclercq G, Kamal M, Giraudon JM, Devassine P, Feigenbaum L, et al. (1996) Study of the preparation of bulk powder tungsten carbides by temperature programmed reaction with CH_4+ H_2mixtures. Journal of Catalysis 158(1): 142-169.
19. Atkins P, Jones L (2001) Principles of chemistry: questioning modern life and the environment.
20. Avrami M (1939) Kinetics of phase change. The Journal of Chemical Physics 7: 1103-1112.
21. Sávio R, Costa DA (2017) Master dissertation synthesis, characterization and kinetic evaluation of obtaining wc-co through gas – solid reaction natal.
22. Cetinkaya S, Eroglu S (2017) Thermodynamic analysis and synthesis of fine WC powder in the WO_3-CH_4-H_2 system using excessive CH_4. JOM 69: 2003-2008.
23. Ma J, Zhu SG (2010) Direct solid-state synthesis of tungsten carbide nanoparticles from mechanically activated tungsten oxide and graphite. International Journal of Refractory Metals and Hard Materials 28: 623-627.